LUND UNIVERSITY

Ammonia adsorption on iron phthalocyanine on Au(111): Influence on adsorbate-substrate coupling and molecular spin.

Isvoranu, Cristina; Wang, Bin; Ataman, Evren; Schulte, Karina; Knudsen, Jan; Andersen, Jesper N; Bocquet, Marie-Laure; Schnadt, Joachim

Link to publication

Total number of authors:
8

Ammonia adsorption on iron phthalocyanine on Au(111): Influence on adsorbate–substrate coupling and molecular spin

Cristina Isvoranu,[1] Bin Wang,[2] Evren Ataman,[1] Karina Schulte,[3] Jan Knudsen,[1] Jesper N. Andersen,[1] Marie-Laure Bocquet,[2] and Joachim Schnadt[1,a)]

[1]*Division of Synchrotron Radiation Research, Department of Physics, Lund University, Box 118, 221 00 Lund, Sweden*
[2]*Laboratoire de chimie, Ecole normale supérieure de Lyon, 46, Allée d'Italie, 69364 Lyon Cedex 07, France*
[3]*MAX-lab, Lund University, Box 118, 221 00 Lund, Sweden*

The adsorption of ammonia on Au(111)-supported monolayers of iron phthalocyanine has been investigated by x-ray photoelectron spectroscopy, x-ray absorption spectroscopy, and density functional theory calculations. The ammonia-induced changes of the x-ray photoemission lines show that a dative bond is formed between ammonia and the iron center of the phthalocyanine molecules, and that the local spin on the iron atom is quenched. This is confirmed by density functional theory, which also shows that the bond between the iron center of the metalorganic complex and the Au(111) substrate is weakened upon adsorption of ammonia. The experimental results further show that additional adsorption sites exist for ammonia on the iron phthalocyanine monolayer. © *2011 American Institute of Physics*. [doi:10.1063/1.3563635]

I. INTRODUCTION

Phthalocyanines are synthetic aromatic compounds with planar structure, formed from four isoindole units linked together through nitrogen atoms. They can be metal free or a metal atom can be encapsulated in the center [cf. Fig. 1 for the molecular structure of iron phthalocyanine (FePc)]. Phthalocyanines have a structure similar to that of the naturally occurring porphyrins, which are important catalytic compounds in cell metabolism. For applications in nanotechnology and chemistry, phthalocyanines have great potential because of their high thermal (up to around 500 °C) and chemical stability (especially under highly oxidative conditions such as in concentrated sulphuric acid media),[1] and because they are rather inexpensive and easy to synthesize on a large scale. On solid supports, phthalocyanines and phthalocyanine derivatives form ordered monolayer structures.[2–7] Such monolayers are promising candidates for novel catalytic[8–12] and gas sensing applications.[13–26] Their function will depend critically on the molecular electronic structure, which for phthalocyanines containing certain transition metals (such as Cr, Mn, Fe, Co) is quite complex with an open shell structure of the *d* orbitals and a number of energetically close-lying electronic states. These states can easily be modified by, e.g., changes in the structure of the support surface and the addition of molecular functional groups, but also, as pursued here, by the adsorption of further ligands. For example, it was previously shown that modifications of the molecule–substrate interaction play a key role in changing the magnetic properties of the molecules[27–29] as well as their surface diffusivity.[30]

The present study reports on the effect of adsorption of ammonia (NH_3) on monolayers of iron phthalocyanine (FePc) on a Au(111) support investigated by x-ray photoelectron spectroscopy (XPS), soft x-ray absorption spectroscopy (XAS), and density functional theory (DFT). Our findings reveal significant changes in the electronic and geometric properties of FePc as a result of the coordination of ammonia to the iron site of the FePc molecule. The adsorption of ammonia leads to a weakening of the FePc–Au(111) interaction, and the ligand field produced by the ammonia results in a spin quench on the FePc molecule. The results demonstrate the possibility to modify both the local spin on the iron atom and the coupling strength of the FePc molecular network to the supporting Au(111) surface by controlled adsorption/desorption of molecular ligands. These results fit in well with previous studies, which have shown the possibility of tailoring the electronic structure of metal atoms and complexes by ligand attachment[31–34] and atom-by-atom manipulation.[35]

In addition, we find evidence for adorption of NH_3 in other sites of the FePc monolayer/Au(111) system. We have used temperature-programmed XPS (TP-XPS) to characterize these adsorbate states and find that NH_3 in these sites is more weakly bonded than when adsorbed on the FePc iron center.

II. EXPERIMENTAL

The XPS and XAS experiments were carried out at beam line I311 (Ref. 36) of the Swedish National Synchrotron Radiation Facility MAX-lab in Lund. The beam line is equipped with a SCIENTA SES200 electron energy analyzer. The base pressure in the preparation chamber is in the high 10^{-11} mbar range and in the analysis chamber in the mid 10^{-11} mbar range.

The Au(111) single crystal was cleaned by repeated sputtering and annealing cycles. For sputtering 0.5 kV argon ions were used, and for annealing a current was passed through

---

a)Author to whom correspondence should be addressed. Electronic mail: joachim.schnadt@sljus.lu.se.
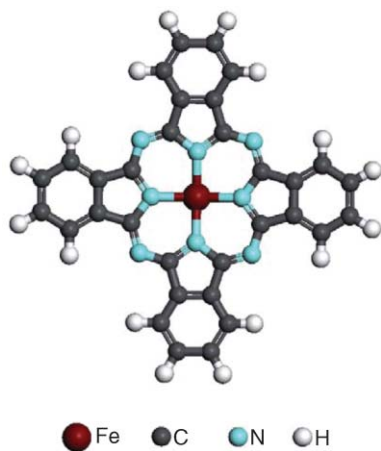
FIG. 1. The molecular structure of the FePc molecule.

the tungsten wire holding the crystal until the temperature reached $500\,^\circ$C. The sample was kept at $500\,^\circ$C for 10 min. Thin iron phthalocyanine films were prepared by vacuum sublimation onto the Au(111) substrate kept at room temperature. The films were then further annealed for several minutes in order to obtain single monolayers. The iron phthalocyanine powder was carefully degassed prior to the experiments by keeping it at temperatures slightly lower than the evaporation temperatures for several days. Before evaporation, the powder was then further degassed by heating it to the evaporation temperature for $\sim$3–4 h. The ammonia adsorption studies were carried out at sample temperatures close to liquid nitrogen temperature. The cooling was achieved by using a helium cryostat and heating the sample to keep the temperature close to 83 K. In order to avoid beam damage of the molecules, the sample was continuously scanned during the measurements at a carefully adjusted and validated speed.

In the x-ray photoelectron spectroscopy experiments photons with energies of 385, 525, and 820 eV were used to record the C $1s$, N $1s$, and Fe $2p$ spectra, respectively. The overall instrumental resolution was 140 MeV for the C $1s$, 180 MeV for the N $1s$, and 280 MeV for the Fe $2p$ photoemission lines. The x-ray photoelectron spectra were normalized with respect to the feature of highest intensity in the spectra. All spectra were calibrated with respect to the Fermi level of the sample. It needs to be pointed out, however, that the Fermi level is not the appropriate reference level for weakly bonded multilayers. It is well known that the vacuum level should be used instead if binding energies are to be considered.[37] The present lack of vacuum level-referenced data does not affect the argumentation below, though, since we interpret the spectral changes in terms of adsorption species independently of the exact binding energies.

The N $1s$ XAS experiments were performed in Auger yield mode. The photon energy scale was calibrated by recording Au $4f$ photoemission spectra excited by first- and second-order light at relevant photon energies. The intensity of the XAS plots was corrected by subtracting a background recorded on the clean Au(111) sample. This treatment eliminated the influence of direct photoemission features of the substrate. Further, a constant low-energy background was

subtracted and the spectra were then normalized to the step at around 25 eV above the absorption edge.[38]

We also carried out TP-XPS experiments, for which we adsorbed ammonia on the FePc/Au(111) sample at 70 K and subsequently recorded N $1s$ x-ray photoelectron spectra on the NH$_3$/FePc/Au(111) sample while heating it slowly. The initial dose of ammonia was 1 L (1 L = 1 Langmuir $= 10^{-6}$ Torr $\times$ s). The sample was heated at a heating rate of $\sim$2 K/min until the ammonia was completely desorbed. From the TP-XPS data we derived a temperature-programmed desorptionlike curve by differentiating the area of the investigated spectral feature as a function of temperature. Desorption energies were estimated from this curve assuming a first-order process and using the formalism of Redhead.[39] The pre-exponential factor was assumed to be 10^{13} Hz.

Previous experience has shown that water contamination is a potential problem when adsorbing NH$_3$ on organometallic compounds under ultrahigh vacuum conditions.[40] O $1s$ x-ray photoelectron spectra measured after NH$_3$ adsorption indeed showed a small oxygen signal. In the supplementary information[41] we evaluate the case with the largest level of water contamination and find it corresponds to approximately one water molecule per three FePc molecules. A minor effect on the results in Sec. III C cannot be excluded.

All DFT calculations were carried out with the VASP package,[42] particularly adapted to model periodic interfaces. The PBE-GGA (Perdew-Burke-Ernzerhof generalized gradient approximation)[43] exchange-correlation potential and the Ceperley–Alder version of the local density approximation (LDA) (Refs. 44 and 45) were both used and electron-core interactions were treated in the projector augmented wave approximation.[46,47] We used a plane-wave cutoff energy of 400 eV and spin polarization. An asymmetric slab was adopted with a four-layer (7×8) Au supercell employed to model the Au substrate and the FePc positioned above one side of the slab. Hydrogen atoms were used to passivate the gold bottom slab, in order to quench the unphysical surface state arising at the reverse side of the metallic slab,[48,49] and to study the influence of the passivation on the molecule adsorption energy. The Brillouin zone was sampled with a single k-point at $\bar{\Gamma}$ because of the large lateral dimensions of the periodic unit cell. The molecule and the uppermost Au layer were free to relax until the self-consistent forces reached 20 MeV/Å. The method of Methfessel–Paxton[50] was used to treat the partial occupancies (0.2 eV smearing width). The Au bulk lattice constant was kept fixed at the calculated value of the uncovered metal, $a = 4.17$ Å with GGA or 4.06 Å with LDA, both in good agreement with experimental values ($a = 4.08$ Å).

It is well known that DFT fails in properly describing dispersion interactions, which are of significant relevance for the binding energy of a large organic molecule such as FePc on a metal surface. The bonding geometry, in contrast, is not very much affected since the potential related to the dispersion forces is very flat.[51] Hence, DFT is an appropriate choice for the theoretical description of our system in most regards, since it does correctly model the interaction between the iron ion and the Au surface, which dominates the bonding geometry. Below we will also argue that the influence of molecular
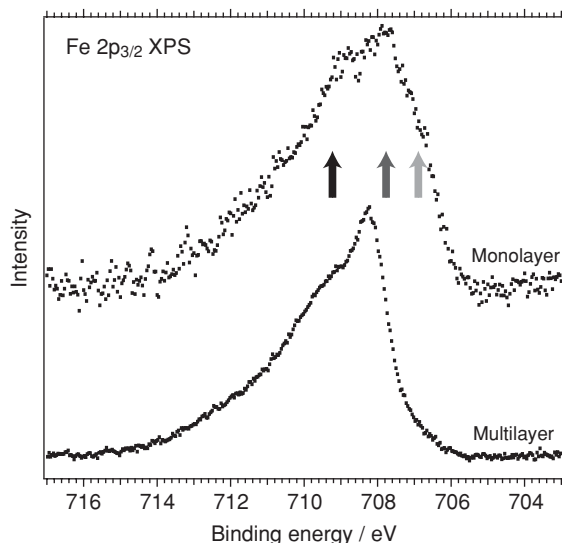
FIG. 2. Fe $2p_{3/2}$ x-ray photoelectron spectra for a monolayer (top spectrum) and a multilayer (bottom spectrum) of FePc on Au(111). A polynomial background was subtracted from both spectra.

deformations given rise to by the neglect of van der Waals forces on the electronic structure is of no further relevance here.

III. RESULTS

A. FePc monolayer on Au(111)

In general, monolayer structures of phthalocyanine molecules are known to adopt flat geometries on most single crystal substrates.[52–57] This is also the case for FePc on Au(111), on which it forms ordered monolayer structures with the planar FePc molecules lying flat on the surface (see supplementary information[41]). The bond between the macrocycle part of the FePc molecules and Au substrate is expected to be largely characterized by van der Waals interactions. As we will show in the following also a weak chemical bond is formed between the FePc and the Au support, namely between the iron ion and the Au surface beneath.

A comparison between the Fe $2p_{3/2}$ photoelectron spectra for a mono- and multilayer of FePc is shown in Fig. 2. The multilayer is here used as a crude approximation for the isolated FePc molecule, under the neglect of intermolecular interactions. For the monolayer we observe a width of the Fe $2p_{3/2}$ photoemission line (FWHM 3.7 eV), which considerably exceeds that observed for the multilayer (FWHM 2.7 eV). This behavior is different from that of the C $1s$ and N $1s$ core levels. For both C $1s$ and N $1s$ core levels the line shapes of the mono- and multilayer spectra are nearly identical; only an overall shift of $\sim$0.4 eV to lower binding energies sets apart the monolayer from the multilayer (see supplementary information[41]). The observation of a rigid shift only in the N $1s$ and C $1s$ spectra and, in contrast, a strong modification of the Fe $2p_{3/2}$ line shape implies coupling of the FePc adsorbates with the Au(111) substrate, which is strongest at the molecular iron center, the width of the $2p_{3/2}$ line being an indicator for the interaction. If one applies the same rigid shift of 0.4 eV found for the N $1s$ and C $1s$ lines to

TABLE I. Theoretical adsorption energies given in eV of the four configurations of FePc on the Au(111) surface. Negative values indicate stable adsorption geometries. For FePc/Au(111) calculations were performed using both GGA and LDA functionals. Further GGA calculations were performed for FePc on a Au(111) slab passivated with hydrogen on the bottom side [GGA(FePc/AuH)].

Functionals	Top	Top rotated	hcp	Bridge
GGA (FePc/Au)	−0.21	−0.25	−0.18	−0.16
LDA (FePc/Au)	−3.07	−3.24	−3.16	−3.18
GGA (FePc/AuH)	−0.23	−0.27	−0.24	−0.21

the multilayer Fe $2p_{3/2}$ spectrum, one finds a peak position at the intermediate, dark gray arrow in Fig. 2. The FePc/Au(111) interaction leads to the occurrence of a pronounced shoulder on the low-binding energy side of this peak (light gray arrow), and in addition, additional intensity is observed on the high binding energy flank as indicated by the black arrow. The appearance of similar spectral features has been observed previously for both phthalocyanines[58] and porphyrins,[59] and has been attributed to different electron configurations in either the ground (charge transfer from substrate and back donation) or core-excited (more/less efficient screening of the core hole) state.[9,59,60] Possibly, the initial and final states effects even occur simultaneously. At high binding energies other unresolved satellites might also play a role.[61] In line with these previous findings, we, therefore, suggest that the monolayer spectrum is composed of three main components with approximate positions as indicated by the arrows in Fig. 2.

More insight into the FePc–Au(111) interface structure is gained from DFT calculations, which have been performed for a number of different FePc configurations which in literature have been proposed to be the most stable ones (Fig. 3).[29,62,63] In the top and top-rotated configurations [Figs. 3(a) and 3(b)] the iron atoms are placed on top of a Au surface atom, in the hcp configuration [Fig. 3(c)] the iron is located on top of a surface hcp site and in the bridge configuration [Fig. 3(d)] on a bridge site. The calculated adsorption energies are presented in Table I. Both GGA and LDA functionals indicate the top-rotated configuration as the most stable one, which agrees with previous scanning tunneling microscopy (STM) and DFT studies.[29,64] The adsorption energies are −0.25 eV (GGA) and −3.24 eV (LDA), the distance between the Fe atom and the Au atom underneath is 2.76 Å (GGA) and 2.65 Å (LDA), respectively, consistent with general LDA versus GGA trends. For the Au slab passivated with hydrogen atoms on the bottom, the same picture also holds true. It should be noted that the energy difference between different configurations is lower than 0.1 eV for GGA and 0.2 eV for LDA, indicating that metastable FePc configurations may occur on the Au (111) surface. The well-known error of absolute DFT binding energies, here using both LDA and GGA, calls for improved functionals, which is beyond the scope of the present report. Since the top-rotated configuration is found to be most stable in calculations using both GGA and LDA functionals and since it also has been observed in earlier STM studies,[29,62] the following discussions will focus on the GGA results of the top-rotated configuration only.

(a) top   (b) top-rotated   (c) hcp

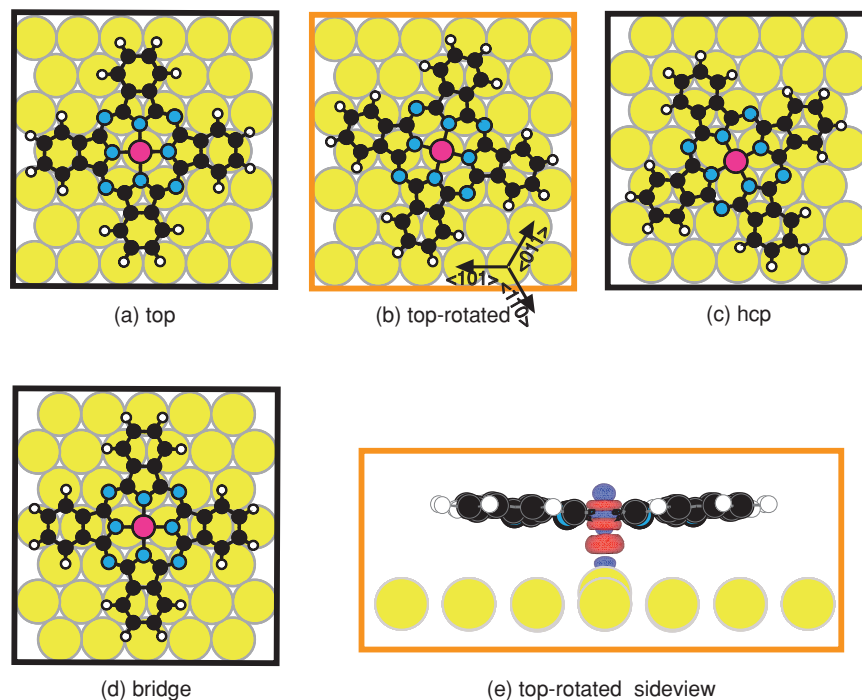(d) bridge   (e) top-rotated sideview

FIG. 3. Optimized structures for FePc/Au(111) from DFT with GGA functional. (a)–(d) Top view of configurations of FePc adsorbed on the Au(111) surface and (e) side view, and charge density difference plot of the most stable configuration, the top-rotated configuration. Red and blue isosurfaces correspond to $\pm 2.0 \times 10^{-2}$ eÅ^{-3}, respectively. The side view shows an interaction between the Fe atom of the FePc molecules and the Au(111) substrate, with a change in the FePc geometry upon adsorption. There is an upward motion of the Au atom beneath the iron atom of approximate 0.4 Å with respect to the average height of the Au(111) surface atoms.

A side view of the calculated top-rotated configuration [Fig. 3(e)] shows that upon adsorption the Au surface atom situated below the Fe is moved upward (0.4 Å). Hence the DFT calculations suggest an interaction between the FePc molecule and the substrate, which is strongest at the molecular iron center in line with the experimental results. The Fe atom and the Au atom share some electron density in the inner space between the Au and Fe atom. As will be discussed later, the bonding is mainly through the d_{z^2} orbital of FePc, which hybridizes with states on the Au atom beneath. For the macrocycle no hybridization with Au state occurs and the bond is of pure van der Waals character.

Before we discuss the adsorption of ammonia on the FePc monolayers, it is appropriate to consider the influence of the valence spin on the Fe $2p_{3/2}$ core-level spectra. It is known from previous work[3] and from our own calculations that the electron distribution in the $3d^6$ valence band of FePc gives two unpaired electrons, due to the fact that the energy of the $3d_{x^2-y^2}$ orbital is significantly enhanced with respect to the $3d_{z^2}$, $3d_{xy}$, $3d_{yz}$, $3d_{xz}$ orbitals ($3d_{x^2-y^2} \gg 3d_{z^2} > 3d_{xy} \approx 3d_{xz, \, yz}$). In consequence, according to Hund's rule only the lowest energy $3d_{z^2}$, $3d_{xy}$, $3d_{yz}$, $3d_{xz}$ states will be populated. In the photoemission process a core hole is created with an angular momentum $\boldsymbol{j}$ and corresponding quantum numbers j and m_j, with $m_j = -3/2$, $-1/2$, $+1/2$, and $+3/2$. The m_j sublevels will split in the effective spin field of the valence d-electrons and the splitting is expected to be of the order of up to some hundreds of meV and to scale approximately linearly with the spin field.[64] Thus, to a large extent the broadening of each of the different Fe $2p_{3/2}$ states of the FePc monolayer on Au(111)—indicated by the arrows in Fig. 2—as well as

the Fe $2p_{3/2}$ multilayer state is determined by the spin of the d-electrons.[65,66] This view is in line with the calculated magnetic moment of 2.02 μ_B (GGA)/2.04 μ_B (LDA) for the isolated FePc molecule and 2.36 μ_B (GGA)/1.41 μ_B (LDA) for the FePc/Au(111) system, consistent with previous theoretical results.[29,63,67]

B. Ammonia adsorption on FePc monolayers: Iron coordination, substrate coupling, and spin

Monolayers of FePc on Au(111), with the characteristics described above, were exposed to different amounts of ammonia at around 83 K sample temperature and studied by XPS. An XAS analysis shows that the FePc molecules remain flat after adsorption of ammonia (see supplementary information[41]). At the same time changes are observed in the N 1s and Fe 2p core-level line shapes. Additional components show up on the high binding energy side of the FePc N 1s photoemission peak at around 398.2 eV (Fig. 4). As expected, the intensity of ammonia-related peak at high binding energy increases with increasing amounts of ammonia. Also the structure of the Fe $2p_{3/2}$ is changed significantly by adsorption of ammonia (Fig. 5). The broad multiplet structure characteristic for the monolayer shows a significant decrease in width due to the reduction in intensity of the component at highest binding energies and a narrowing of the middle component as discussed below. The changes in the Fe 2p core-level spectra and part of the changes in the N 1s spectra are the result of the formation of a coordinate bond between the ammonia lone pair orbital and empty valence states on the iron. In addition, there exist additional ammonia adsorbate species, which give
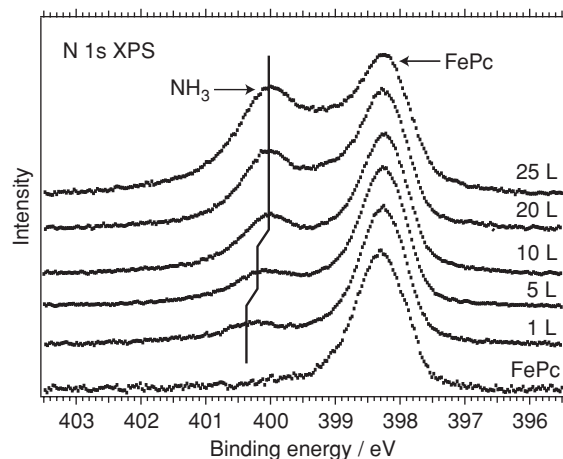
FIG. 4. N 1s photoelectron spectra of one monolayer of FePc on Au(111) before and after adsorption of different amounts of ammonia (up to 25 L as indicated). A polynomial background was subtracted from the spectra. The bottom spectrum represents the N 1s photoelectron spectrum for the FePc monolayer. Ammonia adsorption results in the appearance of the high binding energy peak.
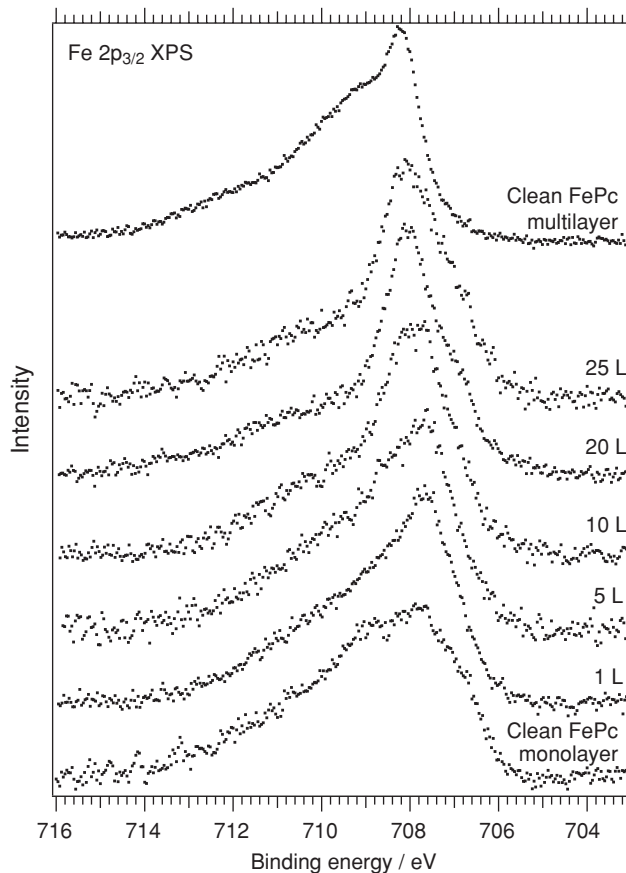

FIG. 5. Fe 2$p_{3/2}$ photoelectron spectra of one monolayer of FePc on Au(111) before and after the adsorption of increasing amounts of ammonia. A polynomial-type background was subtracted from the spectra. The spectrum at 20 L corresponds to the iron saturation coverage, meaning that for this particular coverage all the Fe centers in the monolayer are bound to ammonia ligands. The top spectrum was obtained on a clean FePc multilayer. All spectra have been normalized to their areas.

rise to the remaining intensity of the ammonia N 1s peak. As a result of the small nominal surface coverage of the iron ions (around 3.3% of a monolayer[62]), at larger NH_3 doses the N 1s intensity of the iron-bonded NH_3 is actually dominated by the intensity of these other NH_3 species, which will be discussed in some more detail in Sec. III C of the paper. Here it is the iron-coordinated ammonia species which is of central interest. The reason is that the coordination results in significant changes of the spin properties on the iron atom, as discussed in the following.

In the Fe 2p photoelectron spectra the width of the Fe 2$p_{3/2}$ line decreases with coverage up to a saturation point corresponding to an ammonia dose of approximately 20 L (while, interestingly, the peak does not shift in binding energy to any significant degree). Above this saturation dose, which we call "Fe saturation coverage", an increase in the amount of ammonia does not affect the shape of the Fe 2p spectrum anymore, although the N 1s spectra in Fig. 4 clearly show a continued adsorption of ammonia even beyond this point. The Fe saturation coverage corresponds to a decoration of all iron centers of the monolayer by ammonia molecules. The observed narrowing of the Fe 2$p_{3/2}$ line is attributed to (a) a reorganization of the d orbitals such that the previously paramagnetic ground state of isolated FePc ($S = 1$—two lone electrons in two separate orbitals)[68] is replaced by a diamagnetic one ($S = 0$), where the electrons are paired in a single orbital, and (b) decoupling from the substrate—noting, however, that the continued presence of the low-binding energy shoulder in the Fe 2$p_{3/2}$ spectra suggests that the decoupling is not complete. Regarding the spin changes, similar effects on the spin state are known to occur in coordination chemistry[1,69,70] in the presence of additional ligands such as ammonia and have been observed previously for some phthalocyanine coordination compounds.[71,72]

In more detail, we again use the clean multilayer as a crude approximation of the isolated FePc molecule. In Fig. 5 it is seen that the Fe 2$p_{3/2}$ spectra after higher doses of am-

monia (spectra labeled "20 L" and "25 L") fall off much more rapidly at the high binding energy side than the corresponding spectrum obtained on the clean FePc multilayer. The observed narrowing of the Fe 2$p_{3/2}$ line upon ammonia adsorption cannot be explained by a mere removal of the support-induced state at high binding energy marked by the black arrow in Fig. 2. If this was the only effect, the high energy fall off should have a similar shape as the fall off of the multilayer spectrum, which is not influenced by the Au(111) surface. The dramatic change in line shape must instead be a combined effect of quench of the iron ion's 3d spin and decoupling of the iron ion from the Au(111) substrate—with the result of a decreased intensity at high binding energies. In agreement with the above description of the influence of the valence spin on the Fe 2$p_{3/2}$ line shape, the splitting between the different m_j levels of the core hole state is much reduced upon spin quench due to the changed coupling between the core hole and valence electron angular momenta, and, consequently, the Fe 2$p_{3/2}$ intensity at high binding energies is reduced significantly.

The DFT calculations support the idea of bond formation between the ammonia molecule and the iron (Fig. 6) and show that the presence of ammonia decouples the FePc molecules
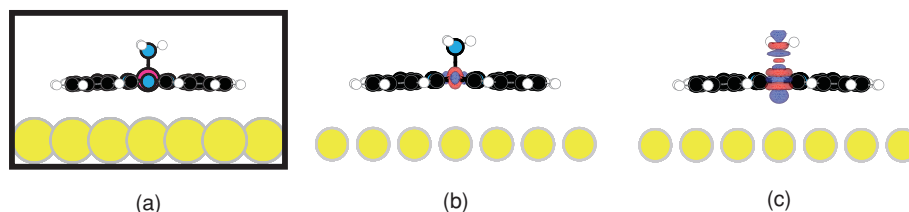
FIG. 6. (a) Side view of ammonia adsorbed on the top-rotated configuration of FePc on the Au(111) surface. The Fe–Au interaction is suppressed due to the formation of the NH_3–Fe bond. (b) Charge density difference plot between FePc and the Au(111) surface. Red and blue isosurfaces correspond to $\pm 2 \times 10^{-2}$ e$Å^{-3}$. (c) Charge density difference between the FePc and the NH_3 molecule. Red and blue isosurfaces correspond to $\pm 3.4 \times 10^{-2}$ e$Å^{-3}$.

from the substrate and quenches the spin on the iron atom. Upon NH_3 coordination the geometry and electronic structure of the FePc molecule are changed as compared to the NH_3-free system. In the calculations the Fe atom is lifted toward the vacuum and the hybridization of the Au and Fe states becomes negligible. The Fe atom is now located 4.04 Å above the Au atom underneath, i.e., at a significantly larger distance than the 2.76 Å found in the calculations for the clean FePc/Au(111). The increase is the net effect of a 0.9 Å lift of the iron atom toward the ammonia adsorbate and a 0.4 Å lowering of the Au atom. At the same time the nitrogen atoms of the FePc move upward by 0.6 Å, while the C and H atoms remain at the same height over the surface.

The increased distance between the iron ion from the Au atom is evidence of the also experimentally observed weakening of the metal ion—substrate bond. While similar substrate bond weakening effects have been found previously for Co-tetraphenylporphyrin on silver[32] and nickel[33] supports, we are not aware of any experimental or theoretical quantification of the increase in distance. We would like to point out, however, that the here provided absolute numbers are not reliable, since the dispersive force interaction between the macrocycle and Au(111) surface, with a definite influence on the absolute adsorbate/surface distance, is not modeled correctly by DFT. This implies also that the observed bending of the FePc molecule might be an artifact of the neglect of van der Waals interactions. As shown further below the molecular bend does not significantly modify the electronic structure of the FePc, and our conclusions remain valid.

The bond between ammonia and iron ion via the Fe $3d$ orbitals induces an electron redistribution, which influences the FePc electronic structure significantly. Similar decoupling effects have previously been reported for porphyrins.[32] Overall, the bond between the FePc iron ions and the NH_3 molecules can be classified as a weak chemisorption bond, in agreement with the notion of a dative bond as suggested by the experimental results. Further, the theoretical results show that the electron redistribution caused by the ammonia ligand leads to a rehybridization of the valence electronic levels and a quench of the spin on the iron atom; the theoretical value for the magnetic moment after ammonia adsorption is about -0.27 μ_B with GGA and 0.14 μ_B with LDA.

Figure 7 illustrates in more detail the changes in the spin and electronic structure upon NH_3 coordination. It shows the spin-polarized projected density of states on the iron atom, with spin-up states depicted as positive and spin-down as negative peaks. Prior to NH_3 adsorption the projected density of states on the d orbitals for the free FePc [Fig. 7(b)] shows that

the d_{xz}, d_{yz}, and d_{xy} orbitals dominate the spin-down resonance at the Fermi level, and the d_{z2} is located at 0.6 and -2.2 eV, in good agreement with Refs. 3 and 66. When FePc is adsorbed on Au(111) [Fig. 7(c)], the resonances close to the Fermi level are broadened due to the hybridization of the electronic states of the iron atom and the Au(111) substrate. The hybridization occurs primarily for the d_{z2} orbitals, which have the strongest z-direction component and which can overlap with the underlying Au(111) states. The spin-down components of d_{xz}, d_{yz}, and d_{xy}, which are very close to the Fermi level in the free FePc molecule, split up into two resonances, d_{xz} and d_{yz}, above the Fermi level, and the d_{xy} below the Fermi level. The interaction between the iron atom and the substrate broadens the d_{z2} orbital, and induces non-negligible charge redistribution. However, the orbital configuration on the iron atom is not modified and, thus, the magnetic moment varies only slightly. As can be seen from Fig. 7(d), the spin is quenched by ammonia adsorption, with almost symmetric positions of spin-up and spin-down resonances, due to charge redistribution on the iron atom.

An issue of importance for the validity of our results is the question whether molecular deformations observed in our calculations and probably given rise to by the DFT-neglect of
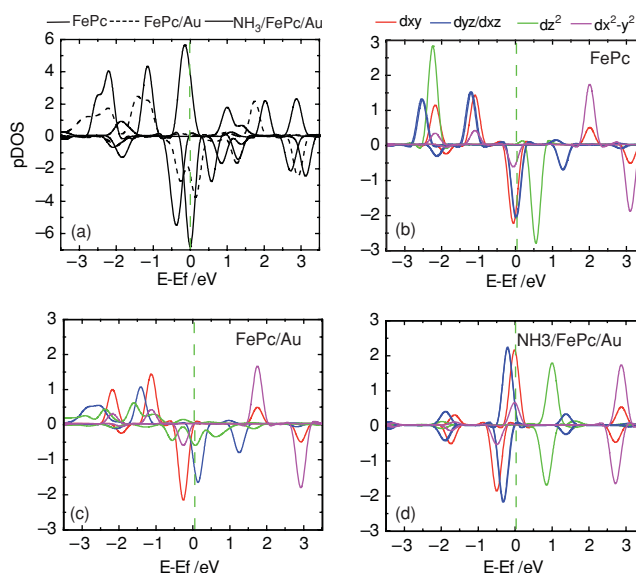

FIG. 7. Projected density of states onto spin-up (positive) and spin-down (negative) states of (a) Fe atom in free FePc, adsorbed FePc (top-rotated configuration) and adsorbed NH_3–FePc. (b) d orbitals of the Fe atom in free FePc molecule. (c) d orbitals of the Fe atom in adsorbed FePc molecule (top-rotated configuration). (d) d orbitals of the Fe atom in adsorbed NH_3–FePc.

van der Waals forces have an influence on the valence electronic structures in Fig. 7 [cf. the slightly bended geometry of FePc in Fig. 3(e)]. In a test run we calculated the Fe 3d electronic structure with all atoms of FePc kept in the optimized positions obtained for the FePc/Au(111) system, but without the Au slab. The resulting electronic structure was compared to that for the free FePc molecule [Fig. 7(b)] and both electronic structures were found to be essentially identical. We, thus, may conclude that the slight deformation of the macrocycle found in the calculations for FePc/Au(111) does not exert any significant influence on the electronic structure and that it is of no relevance for the discussion of our results.

In our calculations we have also probed the adsorption of an amino group (NH_2) on isolated FePc, with the resulting H atom placed on one of the nitrogen atoms of FePc. We found that this system is much less stable than the corresponding system of intact ammonia molecules adsorbed on isolated FePc molecules. Hence, we conclude that a dissociation of ammonia is not favorable.

C. Ammonia adsorption on FePc monolayers: Ammonia species

Since, as discussed above and in the supplementary information,[41] the FePc molecules remain flat on the Au(111) surface upon adsorption of NH_3 and since the Fe 2p x-ray photoelectron spectra in Fig. 5 indicate that there remains some degree of interaction between the FePc iron atoms and the support, we exclude that NH_3 diffuses to an interlayer position between the FePc molecules and the Au(111) support. Thus, we discard the possibility of formation of a FePc(NH_3)$_2$ complex. This implies that, if NH_3 bonded to the FePc centers only, at iron saturation coverage (20 L) one would expect a 1:8 intensity ratio between the N 1s photoemission peaks of NH_3 and FePc in Fig. 4. A larger ratio of 6.4:8 is observed instead, meaning that there exist several competing adsorption sites for ammonia.

In Fig. 8 least-square fits are reported for the N 1s spectra of Fig. 4. In the curve fits we used three peak components (P1, P2, and P3) with the resulting binding energies provided in Table II. The peak at 398.25 eV, labeled P1, corresponds to the N 1s photoemission line related to the nitrogen atoms of the FePc. The peak at around 399 eV labeled P2 is due to the am-
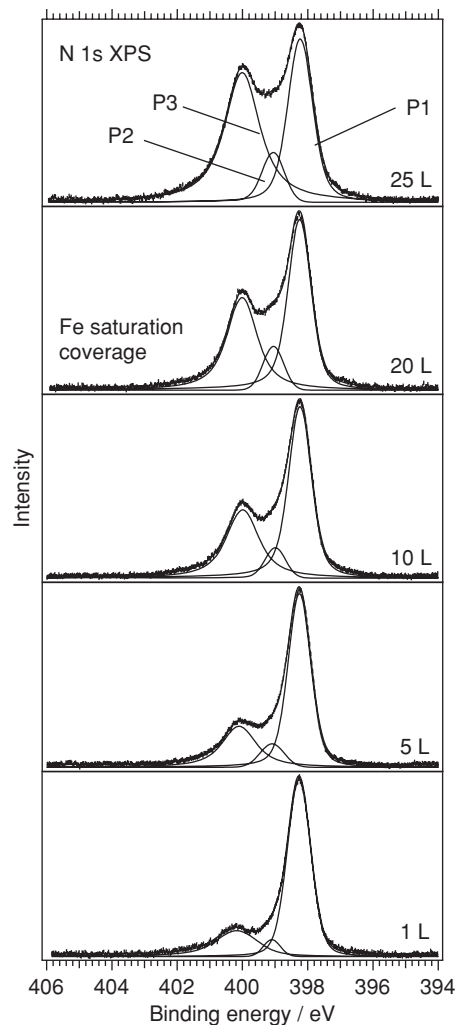

FIG. 8. N 1s photoelectron spectra (experimental data and fits) for the adsorption of 1–25 L of ammonia on one monolayer of FePc on Au(111). The results show several peak components, P1 due to FePc nitrogen, P2 due to ammonia molecules interacting with the gold (Au–NH_3 bond), and P3 related to the ammonia molecules in different sites.

monia molecules interacting with the Au(111) substrate. This we could show by adsorbing ammonia on the clean Au(111) surface, in which case the resulting N 1s line has the same position as that of P2 within the binding energy uncertainty. The highest binding energy peak P3 is related to both the ammonia molecules interacting with the iron and to further ammonia species. That this peak also must be related to other ammonia species besides the iron bonded one is seen from the fact that the P3:P1 intensity ratio at the iron saturation coverage is ~5:8, still significantly higher than the expected 1:8 ratio. P3 continues to grow in intensity for doses higher than those discussed here (not shown), which implies that it eventually represents the NH_3 multilayer signal.

To further study the NH_3 species with contributions to the P3 peak we performed a TP-XPS experiment, the results of which are shown in Fig. 9(a). The starting point for the experiment was a FePc/Au(111) sample, which had been exposed to 1 L of NH_3, i.e., with the NH_3 coverage smaller than the Fe saturation coverage. Slowly heating the sample leads to gradual desorption of the ammonia adsorbates. At around 120 K the FePc N 1s signal is completely recovered and all ammonia

TABLE II. Binding energies of the N 1s components in x-ray photoelectron spectra obtained upon adsorption of increasing amounts of ammonia. The binding energy uncertainty is ±50 MeV.

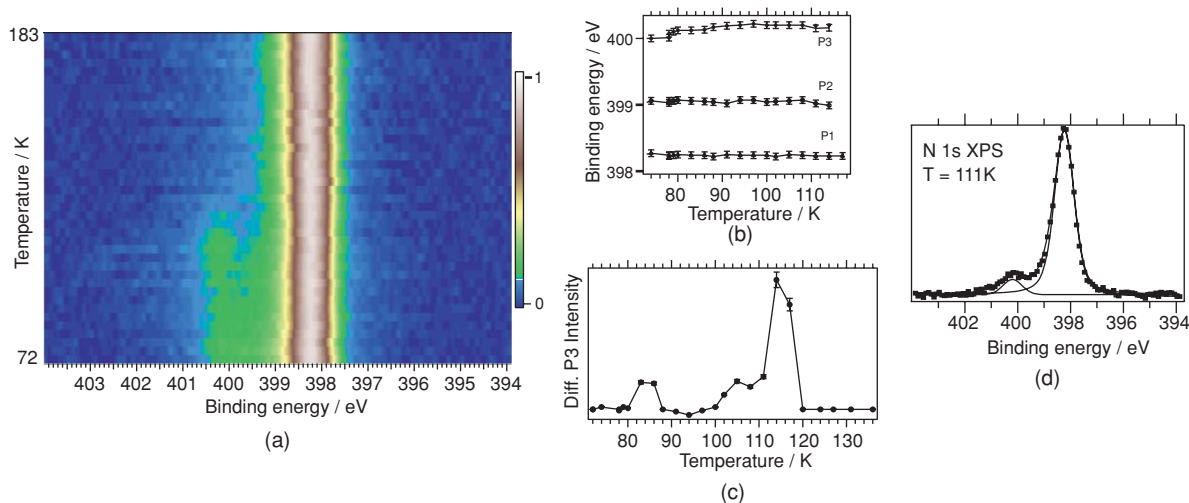| NH$_3$ amount (L)	Binding energy N 1s peak (eV)		
	FePc (P1)	NH$_3$–Au (P2)	NH$_3$–FePc (P3)
1	398.26	399.03	400.26
5	398.25	399.02	400.10
10	398.23	399.00	400.00
20	398.23	399.05	400.02
25	398.24	399.05	400.01

FIG. 9. (a) TP-XPS experiments performed on the Au(111)/FePc/NH_3 sample, after dosing 1 L of NH_3. The sample was gradually heated to temperatures starting with 72 K, and N 1s photoemission spectra were taken at temperatures ranging from 72 up to 183 K. The color scale represents the intensity scale. Ammonia starts desorbing at around 83 K, and at around 120 K all ammonia molecules are desorbed and the N 1s signal of FePc is completely recovered. (b) Evolution of binding energies of P1, P2, and P3 as a function of temperature. (c) Differential of the intensity (considered as the area of the peak) of P3 as a function of temperature, as derived from the TP-XPS scans. The results show three desorption features at 83, 105, and 114 K, respectively, characteristic for P3 ammonia desorption. (d) N 1s photoemission spectrum from the TP-XPS experiment series taken at 111 K, after the most weakly bound ammonia species are desorbed and only the iron coordinated ammonia is present.

molecules are desorbed. All spectra of the TP-XPS run were now curve fitted with three components as above. It is seen from Fig. 9(b) that the binding energies of P1 (FePc nitrogen) and P2 [NH_3/Au(111)] remain constant with increasing temperature within the measurement uncertainty, while the binding energy of P3 increases with temperature. In Fig. 9(c) we show the P3 signal after differentiation with respect to temperature. Three desorption features are seen at 83, 105, and 114 K, which corresponds to estimated adsorption energies of -0.25, -0.31, and -0.34 eV/NH_3 molecule (the sign follows the theory convention of assigning negative adsorption energies to stable states). A temperature of 83 K coincides with the temperature at which the most prominent increase in binding energy of P3 is observed [Fig. 9(b)]. This indicates that it is the particular species related to desorption at 83 K, which is responsible for the lowering in binding energy with NH_3 coverage seen in the N 1s spectra for the stepped adsorption (Table II). We assign the peak at 114 K to desorption of ammonia molecules coordinated to the FePc iron ions, i.e., to the species responsible for the changes in the iron atoms' spin properties. The assignment is based on the fact that we could not find any other more stable ammonia species in the DFT calculations. Chemically it also makes sense since the dative bond between NH_3 and iron is expected to be stronger than any conceivable bond on the macrocycle and isoindole units. Also ammonia molecules hydrogen bonded to other ammonia molecules are expected to have a lower desorption temperature, as has been shown in a previous TPD study.[73] There a multilayer desorption temperature of 100 K was found, and due to a lower heating rate the desorption temperature should be even lower here.

In order to confirm one of the assumptions of our analysis, namely that of an ammonia coverage below the saturation coverage, we consider the particular N 1s spectrum of the TP-XPS series which was recorded at ~111 K [Fig. 9(d)], i.e.,

after desorption of the two more weakly bonded species, but before desorption of the NH_3 molecules bonded to the molecular Fe atoms. At this temperature the intensity ratio of the N 1s peaks related to NH_3 and FePc, respectively, is 1:12, i.e., the number ratio between NH_3 and FePc molecules is 2:3. This is in agreement with the assertion that the Fe saturation has not been reached at a dose of 1 L. In view of the already reached high number of ammonia molecules per FePc it is, however, somewhat surprising that a dose of 20 L is needed to accomplish saturation. In this context it may be noted that the different adsorption states observed in the TP-XPS data in Fig. 9(d) are occupied simultaneously, as can be seen from the Fig. 4 showing the N 1s spectra for the stepped adsorption. This behavior is unexpected, since, from a thermodynamic point-of-view, the adsorption energies as estimated from the desorption curve would suggest a sequential filling of the different sites in order of energy. This implies that the Fe site with a desorption feature at 114 K should be filled first, and below iron saturation it should be the only site which is filled, in contrast to what is observed. Possibly, this issue can be resolved by considering the diffusion characteristics. In general, the diffusion of small molecules on organometallic remains highly unexplored. However, there exists one theoretical study of diffusion of NO on FePc, which predicts diffusion barriers on the order of ~50%–100% of the desorption barrier.[74] Applied to our case and noting that at adsorption $T = 70$ K, which corresponds to $k_B T = 6$ MeV, much smaller than the estimated desorption energies, this suggests a limitation of diffusion of NH_3 on FePc. A similar argument might apply for diffusion from any second-layer NH_3 on the Au(111) surface to the FePc. In any case, further theoretical and experimental work will be necessary to either confirm or discard this diffusion hypothesis.

Likewise, further work will be necessary to conclusively and finally assign all different ammonia species. As has been

mentioned in Sec. II a small water contamination on the level of less than one water molecule per three FePc molecules occurs during ammonia dosage, and this presence of water might have affected the results. In particular the lower temperature desorption observed in the TP-XPS spectra might in part stem from the influence of the water contamination.

IV. CONCLUSIONS

The electronic and geometric structure of FePc monolayers on a Au(111) substrate and the adsorption of ammonia on FePc have been investigated in a combined electron spectroscopy and density functional theory study. The FePc monolayers adsorb in a flat geometry, with the iron atoms forming a weak covalent bond to the Au(111) support. The N 1s and Fe 2p photoemission spectra show significant changes upon ammonia adsorption as a result of the coordination of ammonia to the iron centers of the FePc molecules. We also found several other ammonia adsorbate species, both on the Au(111) surface and the FePc molecules. The exact nature of the additional ammonia species, apart from the ammonia coordinating to the iron ions, is still in need of clarification and further experimental and theoretical investigations will be necessary. The coordination of ammonia to the Fe centers of the macrocycles decouples the FePc molecules from the substrate and quenches the local spin on the iron atom, changing the open valence shell structure of the iron into a closed shell structure. The spin quench on the iron atom paves an efficient and reversible way to manipulate the spin state, quenching it by adsorption and recovering by thermal desorption. In the same way, the coupling between the FePc molecules and the Au(111) support can be manipulated by adsorption and desorption of ammonia.

ACKNOWLEDGMENTS

[1] L. R. Milgrom, *The Colours of Life: An Introduction to the Chemistry of Porpryrins and Related Compounds* (Oxford University Press, New York, 1997).

[2] N. Papageorgiou, E. Salomon, T. Angot, J. M. Layet, L. Giovanelli, and G. L. Lay, Prog. Surf. Sci. **77**, 139 (2004).

[3] X. Lu and K. W. Hipps, J. Phys. Chem. B **101**, 5391 (1997).

[4] M. Takada and H. Tada, Chem. Phys. Lett. **392**, 265 (2004).

[5] K. Nilson, J. Åhlund, B. Brena, E. Göthelid, J. Schiessling, N. Mårtensson, and C. Puglia, J. Chem. Phys. **127**, 114702 (2007).

[6] Z. H. Cheng, L. Gao, Z. T. Deng, Q. Liu, N. Jiang, X. Lin, X. B. He, S. X. Du, and H.-J. Gao, J. Phys. Chem. C **111**, 2656 (2007).

[7] H. Peisert, T. Schwieger, J. M. Auerhammer, M. Knupfer, M. S. Golden, J. Fink, P. R. Bressler, and M. Mast, J. Appl. Phys. **90**, 466 (2001).

[8] T. Abe, K. Nagai, K. Sekimoto, A. Tajiri, and T. Norimatsu, Electrochem. Commun. **7**, 1129 (2005).

[9] Y. Lu and R. G. Reddy, Int. J. Hydrogen Energy **33**, 3930 (2008).

[10] J. C. Obirai and T. Nyokong, J. Electroanal. Chem. **600**, 251 (2007).

[11] M. Toledo, A. M. S. Lucho, and Y. Gushikem, J. Mater. Sci. **39**, 6851 (2004).

[12] S. Baranton, C. Coutanceau, C. Roux, F. Hahn, and J.-M. Léger, J. Electroanal. Chem. **577**, 223 (2005).

[13] M. I. Newton, T. K. H. Starke, M. R. Willis, and G. McHale, Sens. Actuators B **67**, 307 (2000).

[14] X. Ma, H. Chen, M. Shi, G. Wu, M. Wang, and J. Huang, Thin Solid Films **489**, 257 (2005).

[15] K. C. Ho and Y. H. Tsou, Sens. Actuators B **77**, 253 (2001).

[16] C. J. Liu, J. J. Shih, and Y. H. Ju, Sens. Actuators B **99**, 344 (2004).

[17] S. Chakane, A. Gokarna, and S. Bhoraskar, Sens. Actuators B **92**, 1 (2003).

[18] J. C. Buchholz, Appl. Surf. Sci. **1**, 547 (1978).

[19] K. Morishige, S. Tomoyasu, and G. Iwano, Langmuir **13**, 5184 (1997).

[20] L. Alagna, A. Capobianchi, A. M. Paoletti, G. Pennesi, G. Rossi, M. P. Casaletto, A. Generosi, B. Paci, and V. R. Albertini, Thin Solid Films **515**, 2748 (2006).

[21] S. Dogo, J. P. Germain, C. Maleysson, and A. Pauly, Sens. Actuators B **8**, 257 (1992).

[22] T. A. Jones and B. Bott, Sens. Actuators **9**, 27 (1986).

[23] Y. L. Lee, C. Y. Sheu, and R. H. Hsiao, Sens. Actuators B **99**, 281 (2004).

[24] S. Singh, S. K. Tripathi, and G. S. S. Saini, Mater. Chem. Phys. **112**, 793 (2008).

[25] J. Spadavecchia, G. Ciccarella, and R. Rella, Sens. Actuators B **106**, 212 (2005).

[26] V. Vrkoslav, I. Jelinek, M. Matocha, V. Kral, and J. Dian, Mater. Sci. Eng. C **25**, 645 (2005).

[27] N. Tsukahara, K. Noto, M. Ohara, S. Shiraki, N. Takagi, Y. Takata, J. Miyawaki, M. Taguchi, A. Chainami, S. Shin, and M. Kawai, Phys. Rev. Lett. **102**, 167203 (2009).

[28] H. Wende, M. Bernien, J. Luo, C. Sorg, N. Ponpandian, J. Kurde, J. Miguel, M. Piantek, X. Xu, P. Eckhold, W. Kuch, K. Baberschke, P. M. Panchmata, B. Sanyal, P. M. Oppeneer, and O. Eriksson, Nature Mater. **6**, 516 (2007).

[29] L. Gao, W. Ji, Y. B. Hu, Z. H. Cheng, Z. T. Deng, Q. Liu, N. Jiang, X. Lin, W. Guo, S. X. Du, W. A. Hofer, X. C. Xie, and H.-J. Gao, Phys. Rev. Lett. **99**, 106402 (2007).

[30] N. Jiang, Y. Y. Zhang, Q. Liu, Z. H. Cheng, Z. T. Deng, S. X. Du, H.-J. Gao, M. J. Beck, and S. T. Pantelides, Nano Lett. **10**, 1184 (2010).

[31] P. Wahl, L. Diekhöner, G. Wittich, L. Vitali, M. A. Schneider, and K. Kern, Phys. Rev. Lett. **95**, 166601 (2005).

[32] K. Flechtner, A. Kretschmann, H. P. Steinrück, and J. M. Gottfried, J. Am. Chem. Soc. **129**, 12110 (2007).

[33] C. Wäckerlin, D. Chylarecka, A. Kleibert, K. Müller, C. Iacovita, F. Nolting, T. A. Jung, and N. Ballav, Nat. Commun. **1**, 61 (2010).

[34] C. Isvoranu, B. Wang, K. Schulte, E. Ataman, J. Knudsen, J. N. Andersen, M.-L. Bocquet, and J. Schnadt, J. Phys.: Condens. Matter **22**, 472002 (2010).

[35] N. Néel, J. Kröger, R. Berndt, T. O. Wehling, A. I. Lichtenstein, and M. I. Katsnelson, Phys. Rev. Lett. **101**, 266803 (2008).

[36] R. Nyholm, J. N. Andersen, U. Johansson, B. N. Jensen, and I. Lindau, Nucl. Instrum. Methods Phys. Res. A **467–468**, 520 (2001).

[37] T. C. Chiang, G. Kaindl, and T. Mandel, Phys. Rev. B **33**, 695 (1986).

[38] J. Schnadt, J. Schiessling, J. N. O'Shea, S. M. Gray, L. Patthey, M. K. J. Johansson, M. Shi, J. Krempasky, J. Åhlund, P. G. Karlsson, P. Persson, N. Mårtensson, and P. A. Brühwiler, Surf. Sci. **540**, 39 (2003).

[39] P. A. Redhead, Vacuum **12**, 203 (1962).

[40] K. Flechtner, A. Kretschmann, L. R. Bradshaw, M. M. Walz, H. P. Steinrück, and J. M. Gottfried, J. Phys. Chem. C **111**, 5821 (2007).

[41] See supplementary material at http://dx.doi.org/10.1063/1.3563635 for description of experimental evidence.

[42] G. Kresse and J. Furthmüller, Phys. Rev. B. **54**, 11169 (1996).

[43] J. P. Perdew, K. Burke, and M. Ernzerhof, Phys. Rev. Lett. **77**, 3865 (1996).

[44] J. P. Perdew and A. Zunger, Phys. Rev. B. **23**, 5048 (1981).

[45] D. M. Ceperley and B. J. Alder, Phys. Rev. Lett. **45**, 566 (1980).

[46] P. E. Blöchl, Phys. Rev. B **50**, 17953 (1994).

[47] G. Kresse and D. Joubert, Phys. Rev. B **59**, 1758 (1999).

[48] N. G. Lakunza, Ph.D. dissertation, University of the Basque Country, 2008.

[49] N. G. Lakunza, I. F. Torrente, K. J. Franke, N. Lorente, A. Arnau, and J. I. Pasqual, Phys. Rev. Lett. **100**, 156805 (2008).

[50] M. Methfessel and A. T. Paxton, Phys. Rev. B **40**, 3616 (1989).

[51] M. Mura, A. Gulans, T. Thonhauser, and L. Kantorovich, Phys. Chem. Chem. Phys. **12**, 4759 (2010).

[52] V. Oison, M. Koudia, M. Abel, and L. Porte, Phys. Rev. B **75**, 035428 (2007).

[53] A. Scarfato, S.-H. Chang, S. Kuck, H. Brede, G. Hoffmann, and R. Wiesendanger, Surf. Sci. **602**, 677 (2008).

[54]J. Åhlund, J. Schnadt, K. Nilson, E. Göthelid, J. Sciessling, F. Besenbacher, N. Mårtensson, and C. Puglia, Surf. Sci. **601**, 3661 (2007).

[55]M. Lackinger and M. Hietschold, Surf. Sci. **520**, L619 (2002).

[56]L. Scudiero, K. W. Hipps, and D. E. Barlow, J. Phys. Chem. B **107**, 2903 (2003).

[57]K. Nilson, P. Palmgren, J. Åhlund, J. Schiessling, E. Göthelid, N. Mårtensson, C. Puglia, and M. Göthelid, Surf. Sci. **602**, 452 (2008).

[58]K. Schulte, C. Yan, M. Ahola-Tuomi, A. Stróżecka, P. J. Moriarty, and A. N. Khlobystov, J. Phys.: Conf. Ser. **100**, 012017 (2008).

[59]T. Lukasczyk, K. Flechtner, L. R. Merte, N. Jux, F. Maier, J. M. Gottfried, and H. P. Steinrück, J. Phys. Chem. C **111**, 3090 (2007).

[60]S. Hüfner, *Photoelectron Spectroscopy*, 3rd ed. (Springer, Berlin, Heidelberg, 2003), Chap. III.

[61]G. Rossi, G. Panaccione, F. Sirotti, S. Lizzit, A. Baraldi, and G. Paolucci, Phys. Rev. B **55**, 11488 (1997).

[62]Z. H. Cheng, L. Gao, Z. T. Deng, N. Jiang, Q. Liu, D. X. Shi, S. X. Du, H. M. Guo, and H. J. Gao, J. Phys. Chem. C **111**, 9240 (2007).

[63]Z. Hu, B. Li, A. Zhao, J. Yang, and J. G. Hou, J. Phys. Chem. C **112**, 13650 (2008).

[64]G. van der Laan, Phys. Rev. B **51**, 240 (1995).

[65]J. Weissenrieder, M. Göthelid, M. Månsson, H. von Schenck, O. Tjernberg, and U. O. Karlsson, Surf. Sci. **527**, 163 (2003).

[66]F. Sirotti and G. Rossi, Phys. Rev. B **49**, 15682 (1994).

[67]B. Białek, I. G. Kim, and J. I. Lee, Surf. Sci. **526**, 367 (2003).

[68]M. D. Kuz'min, R. Hayn, and V. Oison, Phys. Rev. B **79**, 024413 (2009).

[69]P. A. Cox, *The Electronic Structure and Chemistry of Solids* (Oxford University Press, New York 1987).

[70]J. C. Kotz, P. M. Treichel, and J. M. Townsend, *Chemistry and Chemical Reactivity* (Thomson Brooks/Cole, Belmont, 2009).

[71]T. Kawai, M. Soma, Y. Matsumoto, T. Onishi, and K. Tamaru, Chem. Phys. Lett. **37**, 378 (1976).

[72]G. V. Quedraogo and D. Benlian, J. Chem. Phys. **73**, 642 (1980).

[73]B. D. Kay, K. R. Lykke, J. R. Creighton, and S. J. Ward, J. Chem. Phys. **91**, 5120 (1989).

[74]N. L. Tran and A. C. Kummel, J. Chem. Phys. **127**, 214701 (2007).